BNL-79880-2008-CP

A METHOD FOR THE AUTOMATIC DETECTION OF INSECT CLUTTER IN DOPPLER-RADAR RETURNS

Luke, E., Kollias, P., and Johnson, K.

Presented at the
7th International Symposium on Tropospheric Profiling,
Boulder, CO
June 12-16, 2006

Environmental Sciences Department/Atmospheric Sciences Division

Brookhaven National Laboratory
P.O. Box 5000
Upton, NY 11973-5000
www.bnl.gov

Notice: This manuscript has been authored by employees of Brookhaven Science Associates, LLC under Contract No. DE-AC02-98CH10886 with the U.S. Department of Energy. The publisher by accepting the manuscript for publication acknowledges that the United States Government retains a non-exclusive, paid-up, irrevocable, world-wide license to publish or reproduce the published form of this manuscript, or allow others to do so, for United States Government purposes.

4.20-P

A Method for the Automatic Detection of Insect Clutter in Doppler-Radar Returns

Edward Luke, Pavlos Kollias, Karen Johnson

Brookhaven National Laboratory, Upton, New York, USA

1. Introduction

The accurate detection and removal of insect clutter from millimeter wavelength cloud radar (MMCR) returns is of high importance to boundary layer cloud research (e.g., Geerts et al., 2005). When only radar Doppler moments are available, it is difficult to produce a reliable screening of insect clutter from cloud returns because their distributions overlap. Hence, screening of MMCR insect clutter has historically involved a laborious manual process of cross-referencing radar moments against measurements from other collocated instruments, such as lidar. Our study looks beyond traditional radar moments to ask whether analysis of recorded Doppler spectra can serve as the basis for reliable, automatic insect clutter screening. We focus on the MMCR operated by the Department of Energy's (DOE) Atmospheric Radiation Measurement (ARM) program at its Southern Great Plains (SGP) facility in Oklahoma. Here, archiving of full Doppler spectra began in September 2003, and during the warmer months, a pronounced insect presence regularly introduces clutter into boundary layer returns.

2. Method

The wing and body motions of airborne insects produce Doppler radar spectra with morphologies that, to the trained eye, are often distinguishable from those of clouds. This leads us to consider whether a signal processing methodology can be devised to consistently make this distinction as well. Since many cases exist where morphological differences are less than obvious, we seek a technique that operates on the basis of statistical best estimates. In the boundary layer, the MMCR at the SGP records 256-FFT point Doppler spectra. Neural networks are well suited to these requirements. We use a feed-forward neural network architecture and the back-propagation training algorithm. After training our classifier on 4000 samples from each class (clear, cloud, insect), the processing steps used to classify Doppler spectra are depicted in figure 1. The insects we are dealing with tend to produce clutter concentrated into narrow spectral width peaks with sharp roll-offs and variable Doppler velocity. Often the peaks occur in clusters (figure 2) resulting in highly variable measured Doppler widths.

As input to the neural network, we need a measure of spectrum morphology that is sensitive to sharp roll-offs, but is simultaneously insensitive to Doppler velocities. That is, we seek invariance to peak positions within the Doppler spectrum. To achieve this, we accumulate frequency histograms of spectra's first and second derivatives, anticipating insect histograms to possess characteristic signatures. This information forms the basis for 89% of our input to the neural network. Figure 2 shows the first and second derivatives of a primary peak. We also input scaled measures of reflectivity, spectral width, Doppler velocity, skewness, kurtosis, and a sum of high-pass filtered spectrum values. Finally, we include range gate altitude as a hint to possible altitude dependent insect effects.

3. Results

Figure 3 shows boundary layer reflectivity for May 5, 2005 at the SGP site, overlaid by ceilometer heights in black. This day has a substantial presence of cloud and insects, but separation of the two based on reflectivity is virtually impossible. Figure 4 shows the output of our insect classifier. We will compare this to figure 5, which shows a cloud mask produced by the collection of algorithms known as Active Remote Sensing of Clouds (ARSCL), the state-off-the-art in cloud profiling (Clothiaux et al., 2000). ARSCL processes data from multiple instrument types to derive a best

Presented at the 7th International Symposium on Tropospheric Profiling, Boulder, CO, June 12-16, 2006.

estimate of cloud boundaries. At the start of the day, the insect classifier shows a short-lived cloud layer between 1500 and 2000 meters as well as an underlying insect layer extending from the ground to roughly 1000 meters. The ARSCL mask also shows the cloud, and rejects the insects, as it should. Hours seven through eight see growth of a substantial cloud layer, leading up to drizzle reaching the ground at hour ten. Cloud with several periods of precipitation dominate from here until hour fifteen. Both the classifier and ARSCL mask show general agreement for these features. After hour fifteen (and a short gap in radar data), the cloud ceiling trends upward with the insect classifier showing a persistent insect layer reappearing and extending from the ground to the rising cloud ceiling. Finally, over the last four hours of the day, our classifier shows a thin layer of broken cloud embedded within insects above and below.

During the final three hours of the day, covered by the box labeled "C" in figure 5, there is a problem. The ARSCL mask shows the presence of scatterers, but its quality control flags indicate ambiguity about their type. Referring back to figure 3, the fluctuating ceilometer appears to confirm what our classifier calls a thin layer of broken cloud. It is well recognized in situations such as this that cloud boundaries, especially cloud tops, are difficult to identify. During these last three hours, most of the scatterers within the mask are probably insects. We can use radar polarimetry to support this conclusion as follows. During its periodic polarization modes (M5 and M6), the SGP MMCR transmits a right hand circular (RHC) pulse and receives the backscattered signals via RHC and left hand circular (LHC) channels in parallel to enable dual polarization measurements. We compute the circular depolarization ratio, CDR = $R_{M6} - R_{M5}$, where R_{M5} and R_{M6} are the mode 5 and mode 6 reflectivities in dB. Due to limited channel isolation (13.5 dB between channels), strong scatterers result in leakage to both channels, limiting CDR to around -13.5 dB.

Pulse scattering from spherical cloud droplets has consistent polarization, whereas a random phase shift introduced by irregularly structured targets, such as insects, causes scattering with random polarization. The resulting effect is for returns from cloud droplets to be consistently attenuated and to cluster near the minimum CDR, but for insect returns to produce a mean CDR near zero. To confirm the dominant target shape in the four time-height regions labeled A, B, C, and D of figure 5 we compute CDR frequency distributions for the enclosed range gates. In regions B, C, and D, we restrict the dataset to gates that are covered by the cloud mask and with reflectivity above noise in both polarizations. For region A, with no cloud mask, we use all range gates that are above noise in both polarizations. Figure 6 shows the resulting distributions. Within region "A" there is a tight clustering around zero, confirming our insect classification. Region "B" shows tight clustering around -13.0 dB, close to the ideal attenuation for spherical scatterers. This confirms our cloud/drizzle classification. Region "D" also has a strong peak close to -13.0 dB, supporting our cloud classification. Curve "C", centered at zero, appears to settle the ambiguity over the final three hours of the day. Our classifier's conclusion that primarily insect scatterers occupy region "C" appears to be correct.

4. Conclusions

Uncertainty about the possible presence of insect clutter in cloud profiling Doppler radar returns is a hindrance to boundary layer cloud research in climates and seasons where insects prevail. This is particularly true when cloud layer thicknesses are important. We have developed a new technique that extracts an indication of insect clutter primarily from Doppler spectrum morphologies, mitigating a deficiency in the ability of current profiling methods to accurately locate cloud boundaries in many situations where insects are present.

5. References

Clothiaux, E. E., T. P. Ackerman, G. G. Mace, K. P. Moran, R. T. Marchand, M. A. Miller, B. E. Martner, 2000: Objective determination of cloud heights and radar refectivities using a combination of active remote sensors at the ARM CART sites. *J. Appl. Meteor.*, **39**, 645-665.

Geerts, B., Q. Miao, 2005: The Use of Millimeter Doppler Radar Echoes to Estimate Vertical Air Velocities in the Fair-Weather Convective Boundary Layer, *J. Atmos. Oceanic Technol.*, **22**, 225-246.

Appendix

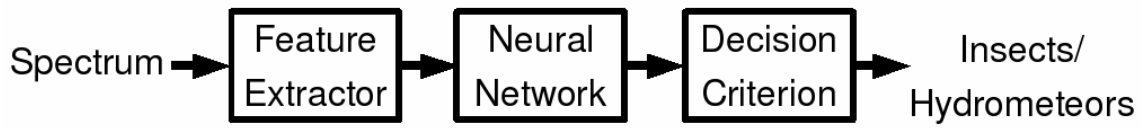

Each Doppler spectrum to be classified is processed by a feature extractor where it is transformed into a new pattern space with reduced dimensionality and a more orthogonal representation of the problem domain. This maximizes neural network efficiency. Feature vectors are then applied to the neural network. The resulting output is a continuous valued vector with a component for each possible classification. These outputs range from 0.0 to 1.0, expressing the confidence of spectrum membership in each class. There is more than one way to interpret the outputs. Our decision criterion implements the "winner-take-all" approach, choosing the class with the highest strength as the spectrum classification.

Figure 1

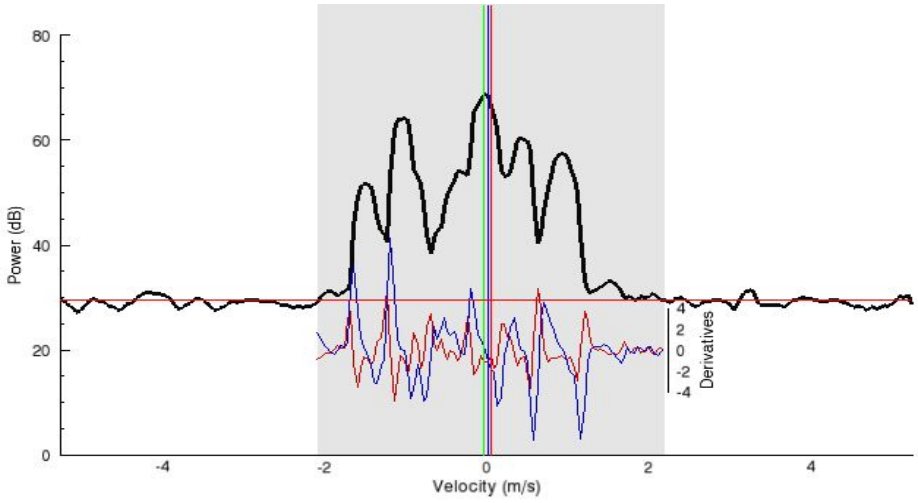

An insect clutter spectrum with multiple peaks. First and second derivatives are shown in blue and red.

Figure 2

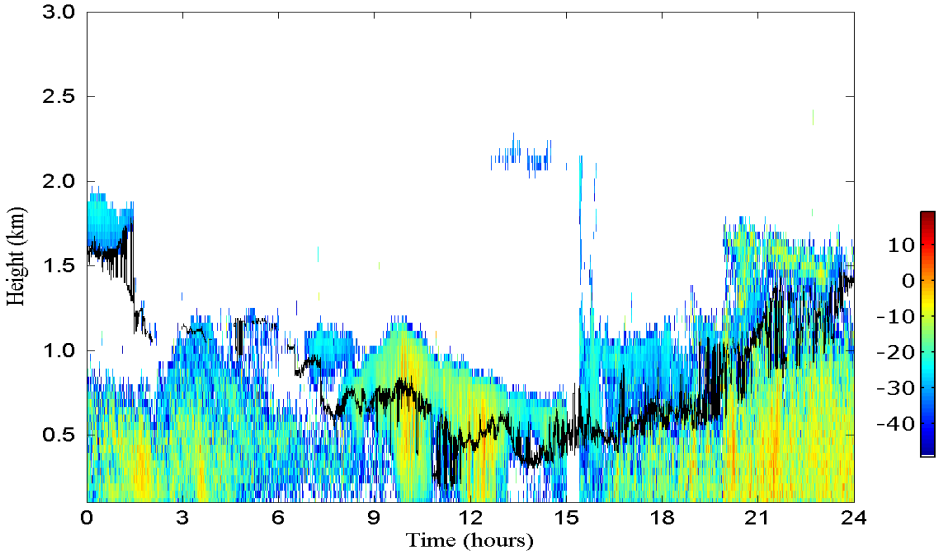

Boundary layer reflectivity for May 5, 2005 at the SGP site, overlaid by ceilometer heights in black. This day has substantial presence of cloud and insects, but separation of the two based on reflectivity is virtually impossible

Figure 3

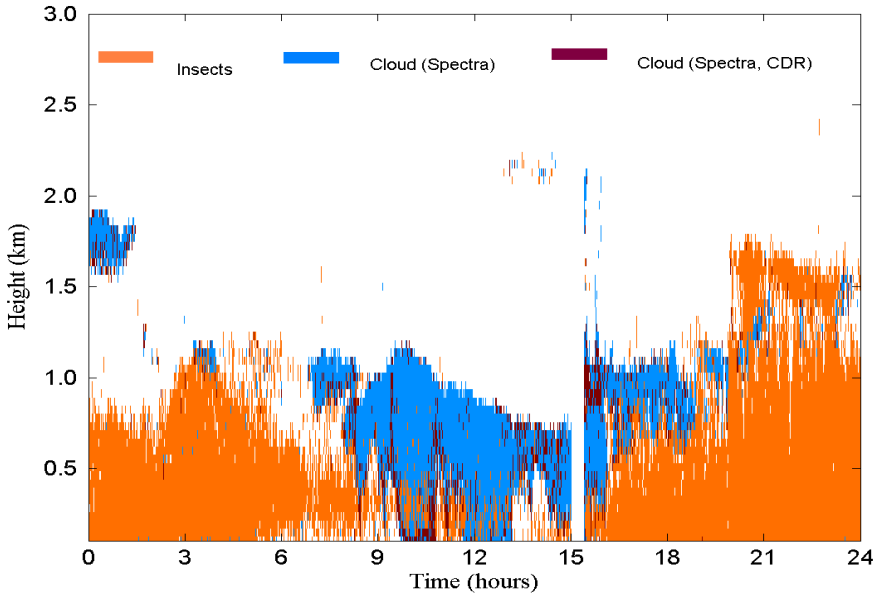

Insect classifier output for May 5, 2005 at the SGP site. Insects are shown in orange and clouds in blue and brown.

Figure 4

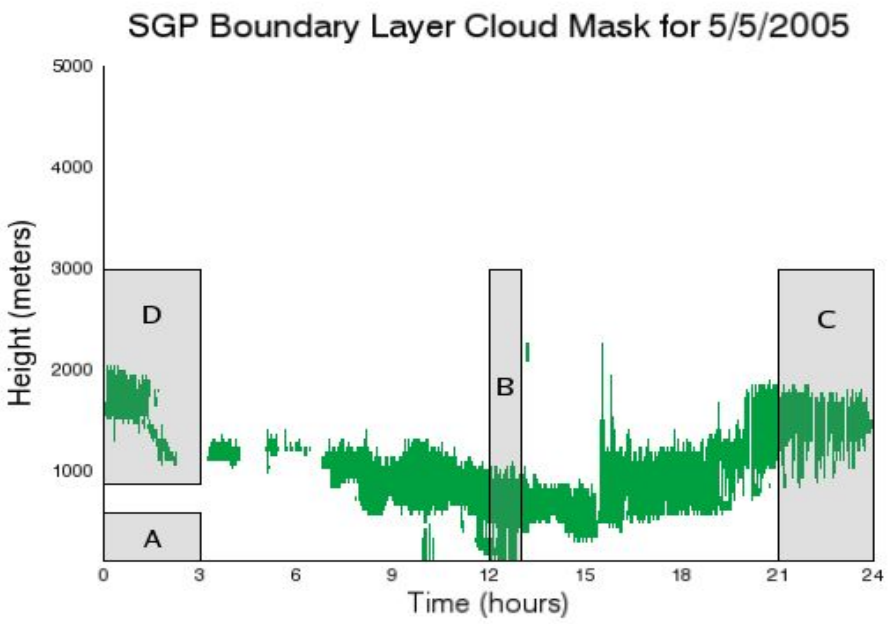

ARSCL Cloud mask for May 5, 2005 at the SGP site derived by processing data from multiple instrument types. This represents the state-off-the-art in cloud profiling.

Figure 5

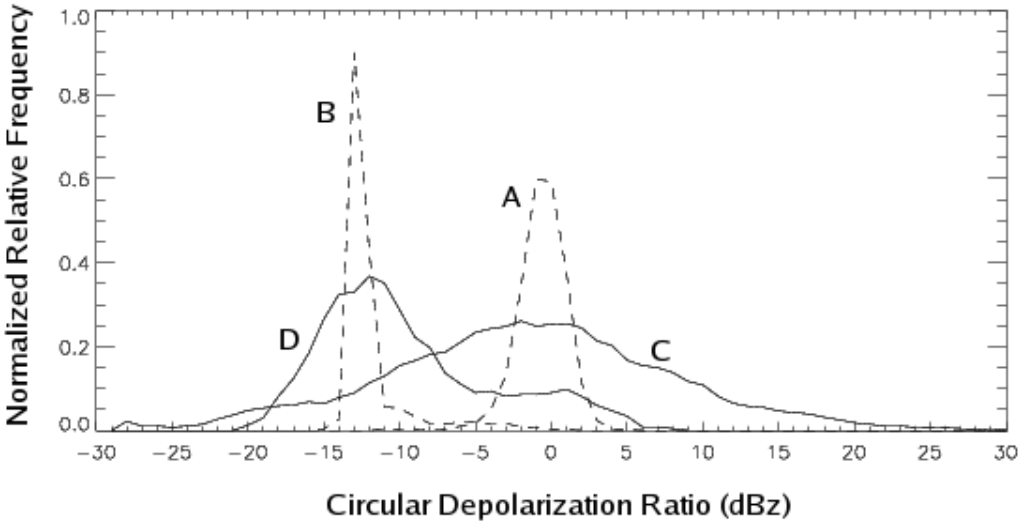

Figure 6